SYNTHESIS AND CHARACTERISATION OF CO DOPED Fe_2O_3 NANOPARTICLES USING *PEDALIUM MUREX LEAF* AND ITS BIOMEDICAL APPLICATION.

A.S. Sakthi athithan[1], D.Renuga[1], Y.Brightson Arul Jacob[2], J.Jeyasundari[2*], sasikala[3]
[1](Research scholar, PG & Research Department of Chemistry, NMSSVN college / Madurai-625019, Tamilnadu, INDIA)
[1] (Assistant professor,PG, Department of Chemistry, Sri Meenakshi college for Women/ Madurai-625002, Tamilnadu, INDIA)
[2] (Assistant professor,PG & Research Department of chemistry, The American college / Madurai -625002, Tamilnadu, INDIA)
[2*](Assistant professor,PG & Research Department of Chemistry, NMSSVN college / Madurai-625019, Tamilnadu, INDIA)
[3](Msc student, Department of chemistry, Fatima college \ Madurai- 625018, Tamilnadu, INDIA)

Abstract
Rapid advancements made in technology, and the drive towards miniaturisation, means that we require reliable, sustainable and cost effective methods of manufacturing a wide range of nanomaterials. Doping of cobalt metal ions in α-Fe2O3 will not only lead to its new technological and industrial applications but also enhance its performance in existing biomedical applications. In the present work, cobalt doped iron oxide nanoparticles was synthesized by co- precipitation method using Pedalium murex leaf extract as reducing and capping agent . The synthesized nanoparticles were characterized by UV and FTIR techniques. The average crystal size of cobalt doped iron oxide nanoparticle was calculated using Debye Scherrer equation, and it was found to be 34 nm, the prepared nanoparticles are in hematite phase, rhombohedral in structure. The surface morphology and elemental analysis of cobalt doped iron oxide nanoparticles was studied using SEM-EDAX. The antimicrobial and anti diabetic activities of synthesized CoIONPs are analysed by disc diffusion, pancreatic α-amy method; thus it shows better results as an anti microbial, anti diabetic agent.

Keywords: CoIONPs, Pedalium murex, SEM-EDAX, XRD, Anti- diabetic, Anti-microbial activity.

1. Introduction

Doping of transition metal ions into Fe_2O_3 can improve the properties of nano crystalline materials by narrowing the energy-band gap and inhibiting electron-hole recombination [1]. The three important crystallographic phases of iron oxide include: 1) magnetite (Fe_3O_4); 2) maghemite (γ- Fe_2O_3) and 3) hematite (α- Fe_2O_3). Among the various materials of iron oxide, especially hematite (α- Fe_2O_3) phase is an important candidate. Hematite (α- Fe_2O_3), also known as ferric oxide, is blood red in colour and is extremely stable at ambient conditions. It is often the end product of other iron oxide transformations. Hematite is a semiconductor material with optical band gap of 2.2 eV [2].Hematite is weakly ferromagnetic at room temperature because of canted spins with a saturation magnetization of 0.4 Am^2/kg [3]. It undergoes a phase transition at 260 K (the Morin temperature TM) to antiferromagnetic state. Above the Neel temperature (~956 K), hematite is paramagnetic. Below 960 K, the Fe^{3+} ions are anitferromagnetically aligned [3].

In order to enhance the magnetic properties of hematite, various dopants have been reported in literature including Ti [4], Co [1], Al [5], Cr [6] etc. Among these dopants cobalt, with electronic configuration of [Ar] $3d^74s^2$ has one more electron than iron, has gained much attention. Cobalt atom donates one d and two s electrons to oxygen that results in remaining six electrons on cobalt. When Co is substituted for Fe with spin down electron the spin down d band gets completely filled with remaining one d-electron residing in spin up band. This results in increase in net magnetization in cobalt doped iron oxide nanoparticles.

The replacement of Fe^{2+} by Co^{2+} or Ni^{2+} does not change essentially the nature of crystallographic structure but its unit cell dimension. The cation distribution in spinels has long been a topic of interest as it affects their magnetic, electric and thermodynamic properties [7-9]. Among the various iron oxides, cobalt doped iron oxide have received recent attention because they possess excellent chemical stability, good mechanical hardness, remarkably high electrical resistivity, and large permeability at high frequency in addition to being cost effective[10-11].

Some of the different ways of preparing the nanoparticles using bottom-up synthesis are: co-precipitation [12], micro emulsion method [13], spray pyrolysis [14], hydrothermal synthesis [15] etc. Recently, great efforts were made to use green and eco-friendly method for synthesis of nanosize materials. These efforts include the use of plant or fruit extracts as surfactant [16]. The plant extracts release a variety of metabolites including carbohydrates, polysaccharides, phenols, amino acids, and vitamins, which can act as capping agents, reducing agents, stabilizing and chelating agents. The use of plant extracts in the synthesis can influence the size, the shape, and the morphology of the nanoparticles. They generate nanoparticles with high dispersity, high stability, and narrow size distribution [17-18].

To enhance the magnetic properties of hematite, we here report synthesis and characterization of cobalt-doped iron oxide using co-precipitation and it also aims to detect the antimicrobial, antidiabetic activity of these nanoparticles.

2. Materials and Methods

Plant source- leaves of *Pedalium murex*

The plant sources were collected from Kodai road, Dindigul District, Tamil Nadu, India.

.

Kingdom	*Plantae*
Division	*Magnoliophyte*
Class	*Magnoliopsida*
Order	*Lamiales*
Family	*Pedaliaceae*
Genus	*Pedalium*
Species	*Pedalium murex L*inn

2.1 Plant description

Traditionally, P. murex was utilized in various ways, either as a whole plant or individual plant parts or sometimes in different special preparations. The leaves are cooked and eaten as a vegetable. In the form of powder, it can be applied locally with butter are used for rheumatic pains [19]. Leaf decoction is used to treat diabetes [20]. Leaves of P. murex are used to treat ulcers, dysuria, Bone fracture, diarrhea and in splenic enlargement [21]. Leaves of Aloevera, P. murex and Bauhinia racemosa crushed together and mixed with water can be given to animals three times a day can relief food poisoning in cattle. An infusion or extract prepared from the different parts of the plant in cold water is used as demulcent, diuretic and also found to be best used in the treatment of disorders of urinary systems such as gonorrhea, dysuria, incontinence of urine and vice versa[22]. The plant is also used by the local people as analgesic and antipyretic activities [23-24].

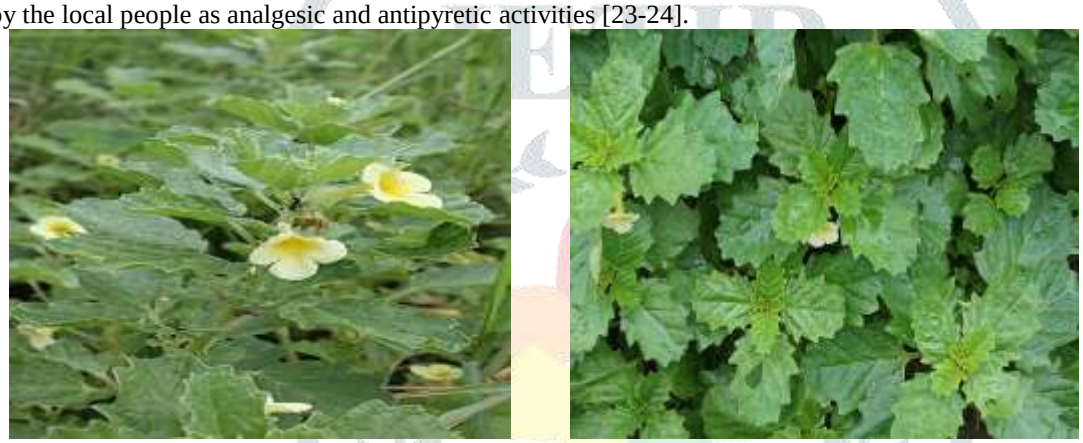

Fig.2.1 Leaf of *Pedalium murex*

2.2 Chemicals required

Stock solutions of $FeCl_3.7H_2O$, $FeSO_4.7H_2O$ and $CoCl_2.6H2O$, NH_4OH.

2.3 Preparation of plant extract

Fresh and healthy leaves were collected and rinsed thoroughly first with tap water followed by distilled water to remove all the dust and unwanted visible particles. Pedalium murex plant leaves were cut into pieces and boiled with 100ml of double distilled water in a 400ml beaker for 30 minutes. The solution is then filtered through Whatman no.1 filter paper. The p^H value of the extract 4.5 is noted. The pure filtered plant extract is stored in a container and refrigerated at 4^0C for further experimental work [25].

2.4 Phytochemical analysis

The results for the phytochemical analysis are shown below

Table 1. Phytochemical analysis of the Pedalium murex leaf

Phytochemicals	Result
Steroid	++
Tannin	++
Flavonoid	++
Phlobatinin	--
Terpenoids	++
Cardial glycosides	++
Reducing sugar	--

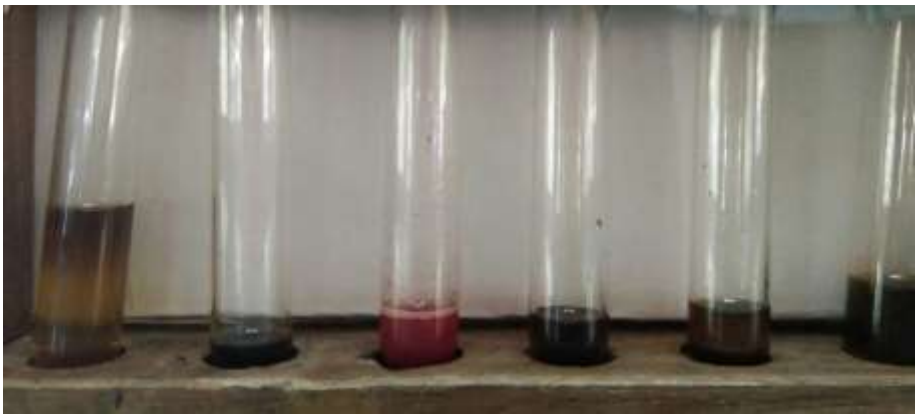

Fig. 2.4 (a) Tests for the presence of phytochemicals in the plant extract

2.5 Synthesis of cobalt doped iron oxide nanoparticles

In our work, Cobalt doped iron oxide nanoparticles were synthesized using green synthesis ecofriendly approach. Aqueous solution of Ferrous Sulphate, Cobalt chloride and Ferric Chloride solution prepared in plant extract is precipitated in 2:1:1 ratio is mixed with 0.2M Cobalt chloride solution, stir the solution well simultaneously with constant stirring , add 0.2 M of $FeCl_3$ solution to the mixture. After 10 minutes of constant stirring the solution is mixed with 0.1 M NH_4OH. This reaction mixture is kept at 85-90^{0}C for 4 hours. The cobalt doped iron oxide nano particle solution thus obtained was purified by repeated centrifugation at 10,000rpm for 10min followed by redispersion. The Nano solution is stored for UV-Vis and FTIR spectroscopic analysis.

Then the solution is centrifuged at 8000 rpm and the colloidal solution is retained. The colloidal solution obtained is then transferred to the petri plate and dried in a hot air oven at 250^{0}C for 3 hours. The dried sample is again calcinated using muffle furnace.

2.6 Disc diffusion method

The standardized inoculums are inoculated in the plates prepared earlier (aseptically) by dipping a sterile in the inoculums removing the excess of inoculums by passing, pressing and rotating the swab firmly against the side of the culture tube above the level of the liquid and finally steaking the swab all over the surface of the medium 3 times rotating the plates through an angle of 60^o c after each application. Finally pass the swab around the edge of the agar surface. Leave the inoculums to dry at room temperature with the lid closed.

The petri dish is divided into parts, in each part, sample disc such as CoIONPs (100µg) (discs are soaked overnight in sample solution) and standard Ciprofloxacin & Flucanazole (10µg), are placed in the plate with the help of sterile forceps. Then petri dishes are placed in the refrigerator at 4^{0}C or at room temperature for one hour for diffusion. Incubate at 37^{0}C for 24 hours. Observe the zone of inhibition produced by different samples. Measure it using a scale and record the average of two diameters of each zone of inhibition.

2.7 Pancreatic α-amy assay

The α-Amy inhibitory activity of cobalt doped iron oxide nanoparicles was performed, according to our former publication [26].Briefly-amy (0.5mg/ml) was incubated with and without synthetic compounds for 10 minutes at 25 ^{o}c. This experiment was performed in 20mM sodium phosphate buffer, P^H 6.9, containing 6mM sodium chloride. After pre-incubation, the starch solution was added and the reaction mixture was incubated for 30 minutes at 25^{o}c.In order to stop the enzymatic reaction, dinitrosalicylic acid was added as the colour reagent and then incubated in a boiling water bath for minutes. After cooling down to the room temperature ,the reaction mixture was then diluted by adding distilled water and the absorbance measured at 540 nm on a T90$^+$ UV-VIS spectrophotometer instrument [PG Instrument Ltd.,UK].The measured absorbance was compared with that of the control experiment and the obtained result were considered as criteria for the percentage of α-amy inhibition[26].In this study, the pharmacological inhibitor ,Acarbose was used as a positive control and the experiment were repeated for at least three times .

2.8 Uv-visible spectroscopy

Samples (1mL) suspension were collected periodically to monitor the completion of bioreduction followed by dilution of the sample with 2ml of deionised water and subsequent scan in UV-Visible (Vis) spectra, between the wave lengths of 300-800nm in a spectrometer (Beckman-Model No.DU-50, Fullerton) having a resolution of 1nm

2.9 Ftir spectroscopy

For the Fourier Transform Infrared (FTIR) spectroscopy analysis the vacuum dried Cobalt doped iron oxide nanoparticles were mixed with Potassium Bromide (KBr) and the spectra were recorded with a Perkin Elmer Spectrum Express version 10,300. The Scanning data were obtained from the average of 47 scans in the range 4000-400cm^{-1} with the resolution of 4cm^{-1}

2.10 Xrd analysis

The Crystal structure of the produced Cobalt doped iron oxide NPs was determined and confirmed by using X-ray diffraction meter (Model PW 1710 control unit Philips Anode Materials Cu, 40 kv, 30 MA, optics Automatic divergence slit) with Cu kv

radiation λ=1.5405A^0 over a wide range of Bragg angles ($30^o \leq 2\Theta \leq 80^o$) . An elemental analysis of the sample was examined by energy dispersive analysis of X-rays with JED-2300 instrument. The crystalline domain size was calculated from the width of the XRD Peaks, assuring that they are free from non uniform strains. The particle size of the prepared samples were determined by using Scherer's equation as follows, $D=0.94\lambda/\beta\cos\Theta$, where λ is the X-ray wavelength, β is the full width at half maximum (FWHM) and Θ is the diffraction a ere D is the average crystalline domain size perpendicular to the reflecting angle

2.11 Scanning Electron Microscopy – Energy Dispersive X-ray Spectrometry (SEM–EDAX) Analysis

The microstructure and composite homogeneity of the obtained samples were investigated using a SEM/EDX scanning microscope JEOL-JSM 64000 LV. Energy dispersive X-ray analysis measurements were performed under standard conditions. The cobalt doped iron oxide nanoparticles were centrifuged at 10,000 rpm for 30 min and the pellet was redispersed in 10 mL ethanol and washed 3 times with sterile distilled water to obtain the pellet. The pellet was dried in an oven and thin films of dried samples (10 mg/mL) were used for compositional analysis.

3. Results and discussion

3.1 Uv-visible spectroscopy

The surface Plasmon resonances (SPR) of synthesized cobalt doped iron oxide nanoparticles have been studied by UV-Vis spectroscopy. After the addition of Pedalium murex leaf extract into the aqueous solution of iron chloride, iron sulphate and cobalt chloride the solution was filled in glass cuvette of path length 10mm and UV-Vis spectral analysis has been done in the range of 300 to 700 nm. Plant extract was used as blank.

UV-Vis absorption spectral study may be assisted in understanding electronic structure of the optical band gap of the material. Absorption in the near ultraviolet region arises from electronic transitions associated within the sample.

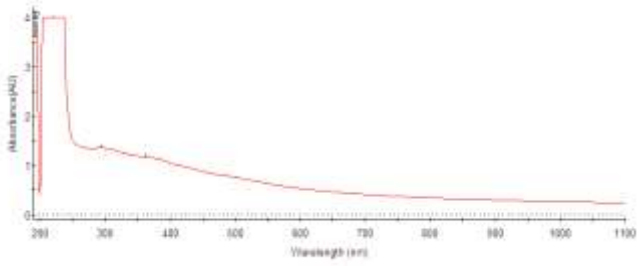

Fig.3.1(a) UV-Visible spectrum of plant extract (Pedalium murex)

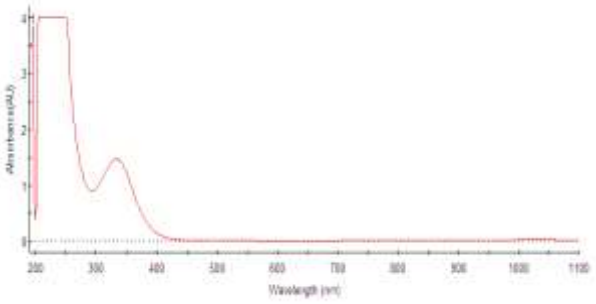

Fig. 3.1(b) UV-Visible spectrum for cobalt doped iron oxide nanoparticles using pedalium murex.

The optical properties of synthesized iron oxide nanoparticles using UV visible spectroscopy were studied and the recorded spectra are shown in figure 3.1(a) and 3.1(b). The optical absorption of cobalt doped iron oxide a nanoparticle of which is measured in a scanning range of wavelength from 300 to 800 nm.

The absorption band around at 361nm by the optical absorption results (27), it is possible to determine band gap energy for the prepared sample.

3.1.1 Band gap calculation

The absorbance peak is related to the band gap energy, and hence using maximum absorbed wavelength, peak wavelength can be converted into band gap energy (27).

This can be converted using Einstein-plank's relation:

$$E = hc / \lambda$$

$$E = 6.626 \times 10^{-34} \times 3 \times 10^{8} / 361.65$$

$$= 3.431 \text{ eV}$$

The obtained band gap energy is 3.431eV and its absorption range occurs about 361.65nm

3.2 Ftir spectroscopy

FT-IR analysis gave the stretching vibrations in the region of 400-4000 cm^{-1} (Fig.5.2). The peak at 3387 cm^{-1} corresponds to the –OH,-NH bond stretching denotes the aqueous phase , 1630 cm^{-1},1384cm^{-1} corresponds to the C=O,C-O bond stretching

denotes the phytochemicals present in the plant extract which stabilize as well as act as a capping agents. The strong peaks at 543 cm^{-1},473cm^{-1} corresponds to the inorganic stretching indicates the iron oxide-NPs. The intensity absorption band at 543cm^{-1} is stronger than at 473cm^{-1} it gives evidence for the formation of Cobalt doped alpha Fe_2O_3 (28)this is agreement with the XRD measurements.

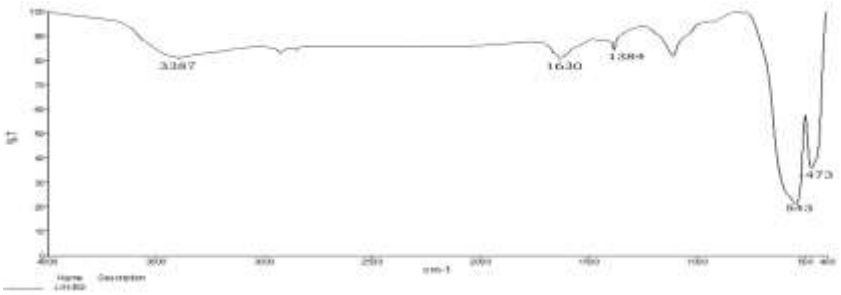

Fig. 3.2 FTIR spectrum of cobalt doped iron oxide nanoparticles

3.3 Xrd analysis

XRD used determine the size of the nanoparticles. The mean size of nano particles is calculated using Debye-Scherrer equation.

The particle size of the prepared samples were determined by using Scherer's equation as follows,

$$D=0.94\lambda/\beta\cos\Theta$$

Where

D is the average crystalline domain size perpendicular to the reflecting planes,

λ is the X-ray wavelength,

β is the full width at half maximum (FWHM)

Θ is the diffraction angle.

The peaks at 2θ values of 24.27, 33.34, 35.80, 41.00, 49.64, 54.18, 62.66, and 64.17 correspond to the lattice planes (012), (104), (110), (113), (024), (116), (214) and (300) respectively. These planes represent the synthesized iron oxide nanoparticles were in hematite phase (α-Fe_2O_3), rhombohedral in structure. It's confirmed at JCPDS #89-8104. The sizes of the nanoparticles obtained were estimated to be 34nm using Debye scherrer equation.

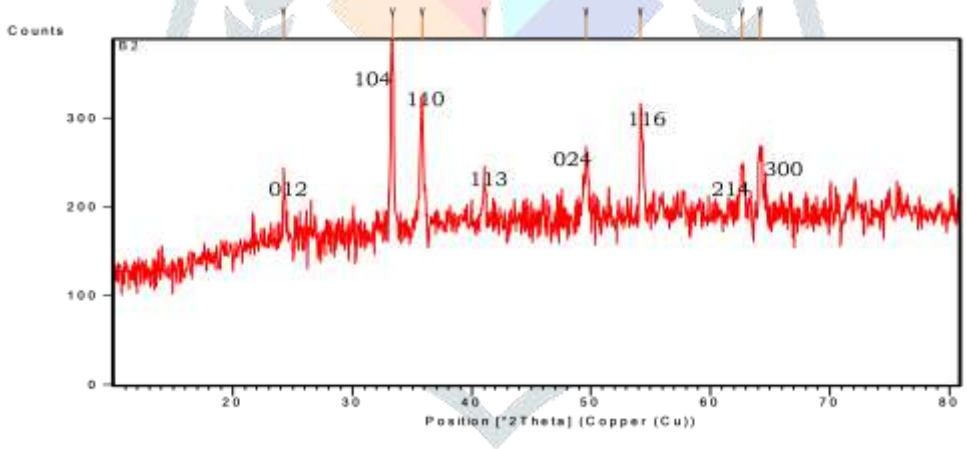

Fig. 3.3 XRD pattern for the cobalt doped iron oxide nanoparticles

3.4 Sem and Edax analysis

The presence of elemental iron oxide can be seen in the graph presented by EDAX, Which indicates the reduction of Cobalt doped iron oxide nanoparticles. The result of EDAX gives a clear idea about the elements present in the biosynthesized nanoparticles. The EDAX profile of cobalt doped iron oxide nanoparticles shows strong signal of the Fe atom indicates the crystalline property as shown in the fig (3.4). The Vertical axis displays the number of X- ray counts while the horizontal axis displays energy in Kev. The optical absorption peak is at 7 Kev which is typical for the absorption of metallic cobalt doped iron oxide nanoparticles. Other than this signal for C, O is observed which may originate from the biomolecules capped to the surface of the cobalt doped iron oxide nanoparticles.

To determine the morphology of the synthesized iron oxide nanoparticles the sample was analysed with scanning electron microscopy (SEM). FeO NPs synthesized using pedalium murex are studied under SEM and shown in fig (3.4).It indicates that FeO NPs formed predominantly and aggregated into larger irregular structure because of the adhesive nature of the nanoparticles. The average diameter of the prepared nanoparticle in solution was about 30 – 80nm.

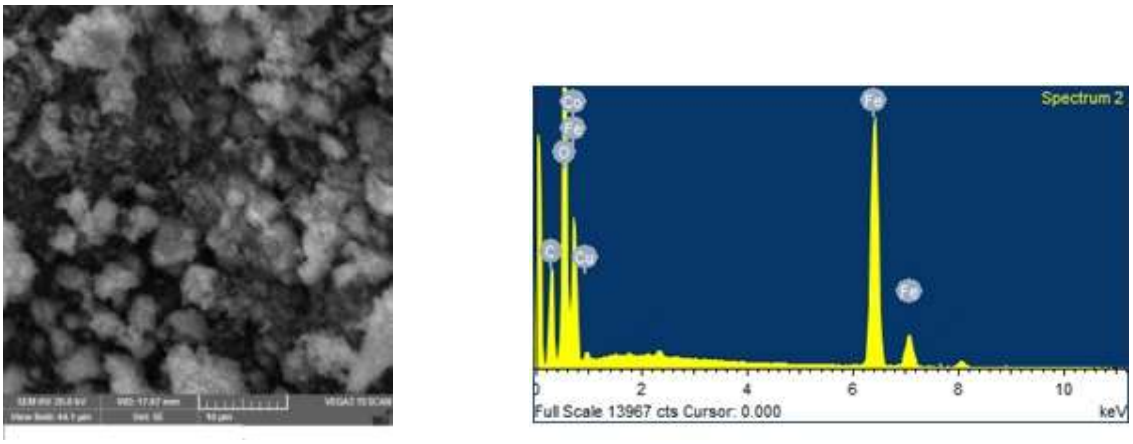

Fig. 3.4 Sem – Edax spectrum of cobalt dopped iron oxide nanoparticles

3.5 Anti-bacterial activity

The anti-bacterial activity was tested by using disc diffusion method against two bacterial species. Among them, one is gram-positive and the other is gram negative such as Staphylococcus aureus and Escherichia coli [29].

Ciprofloxacin is kept as the standard sample and the zone of inhibition is noted.

3.4 (a) 3.4 (b)

Fig.3.4 Inhibition zone of Escherichia coli (a) and Staphylococcus aureus (b)

Table 2- Antibacterial activity of CoIONPs

Organisms	Zone of inhibition	
	Standard Ciprofloxacin [10µg/disc]	Samples [100µg/disc]
Staphylococcus aureus	32	12
Escherichia coli	48	15

3.6 Anti-fungal activity

The synthesized cobalt doped iron oxide nanoparticles were tested against two fungal species i.e. Aspergillus Niger and Candida albicans by disc diffusion assay [30]. Flucanazole, a commercial antifungal drug is kept as the standard sample. The zone of inhibition is noted. CoIONPs exhibit good anti-fungal activity compared to anti-bacterial activity.

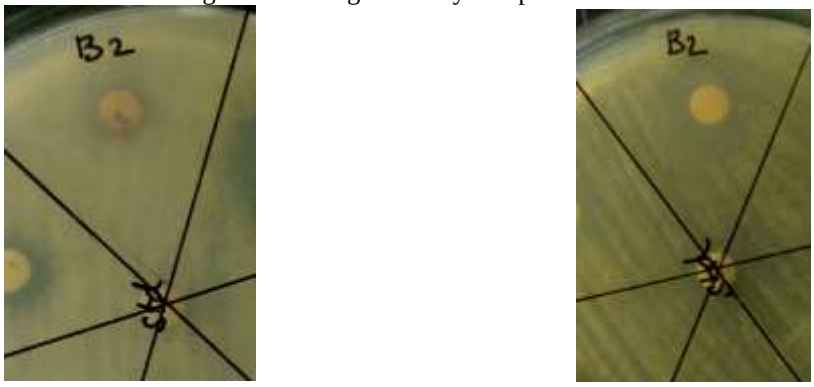

3.5 (a) 3.5 (b)

Fig.3.5 Inhibition zone of Candida albicans (a) and Aspergillus niger (b).

Table 3- Antifungal activity of CoIONPs

Organisms	Zone of inhibition[mm]	
	Standard Flucanazole [10µg/disc]	Sample [100µg/disc]
Aspergillus niger	11	10
Candida albicans	10	9

3.7 Anti diabetic activity

3.7.1 The inhibition activity of cobalt doped iron oxide nanoparticles against α-amy

The anti-diabetic activity was tested by using pancreatic α-amy assay method .Inhibition of α-amy is considered a useful strategy for the treatment of disorders in carbohydrate uptake ,such as diabetes and obesity as well as the dental caries and periodontal disease[28]. Acarbose, a commercial ant diabetic drug is kept as the standard sample and then inhibitory activity of cobalt doped iron oxide nanoparticle is noted.

Fig. 3.6.1 (a) Inhibition activity of Acarbose

Fig 3.6.1 (b) inhibition activity of blank (plant extract

Fig. 3.6.1 (c) Inhibition activity of CoIONPs

Table – 4 Anti diabetic activity of CoIONPs

Concentration	Blank	Standard [Acarbose]	CoIONPs
20	10.12	17.68	15.52
50	15.55	29.32	25.21
100	25.76	50.42	42.23
150	42.23	65.66	61.75
200	63.33	89.98	83.33

4. Conclusion

The present work showed that cobalt doped iron oxide nanoparticles were synthesized by co- precipitation method using *Pedalium murex* as reducing agent .In UV-Vis Analysis, the peak observed at 361nm shows the formation iron oxide nanoparticles and the calculated band gap energy is 3.431eV.FTIR analysis shows that the peaks observed at 543cm^{-1} and 473cm^{-1} concludes the formation of cobalt doped iron oxide nanoparticles.XRD analysis shows that the size of synthesized nanoparticles is 34 nm, the prepared iron oxide nanoparticles are in hematite (α- Fe_2O_3)phase, rhombohedral in structure. The synthesized cobalt doped iron oxide shows good antimicrobial and anti diabetic activity.

5. References

[1]. Suresh, R., Prabu. R., Vijayaraj. A., Giribabu. K., Stephen. A. and Narayanan.V. 2012. Facile synthesis of cobalt doped hematite nanospheres: Magnetic and their electrochemical sensing properties. Materials Chemistry and Physics, 134(2-3): 590-596.

[2]. Monti et al, M. 2012. Magnetism in nanometer-thick magnetite. Physical Review B , 85(2): 020404.

[3]. Bhowmik, R. N. and Saravanan. A. 2010. Surface magnetism, Morin transition, and magnetic dynamics in antiferromagnetic α-Fe2O3 (hematite) nanograins. Journal of Applied Physics, 107(5): 053916.

[4]. Wang, B., Song, Y., Ren, W., Xu, W. and Cui, H. 2009. Low temperature transformation from γ-Fe_20_3 to Ti doped α-Fe_2O_3 nanoparticles through an epoxide assisted sol–gel route. Journal of Sol-Gel Science and Technology., 51(1): 119–123.

[5]. Shinde, S.S., Moholkar, A.V., Kim, J.H. and Rajpure, K.Y. 2011. Structural, morphological, luminescent and electronic properties of sprayed aluminum incorporated iron oxide thin films. Surface and Coating Technology, 205: 3567–3577.

[6]. Yogi, A. and Varshney, D. 2013. Magnetic and structural properties of pure and Cr- doped hematite: α-$Fe_{2-x}Cr_xO_3$ ($0 \leq x \leq 1$), Journal of Advanced Creamics, 2:360-369.

[7]. Goss, C.J. 1988. Saturation magnetisation, coercivity and lattice parameter changes in the system Fe_3O_4- Fe_2O_3, and their relationship to structure. Physics and Chemistry of Minerals, 16(2): 164-171.

[8]. Lenglet, M., and Lefez, B. 1996. Infrared optical properties of cobalt (II) spinels. Solid State Communications, 98(8): 689-694.

[9]. Mendelovici, E., Villalba, R.; Sagarzazu, A. 1998. Distinctive cobalt ferrites prepared by the thermal-transformation alkoxide route . Thermochimica Acta, 318(1-2): 51-56.

[10]. Yootarou**,** Y.,and Satou, M. 1973. High frequency conductivity **i**n cobalt-iron ferrite. Japanese Journal of Applied Physics, 12(7): 998.

[11]. Aldar, B.A., Pinjari, R.K., Burange, N.M., 2014. Electric and dielectric behavior of Ni-Co-Cd Ferrite. Journal of Applied Physics, 6(4): 23–26.

[12]. Gul, I.H., Ahmed, W., Maqsood, A., 2008. Electrical and magnetic characterization of nanocrystalline Ni–Zn ferrite synthesis by co-precipitation route. Journal of Magnetism and Magnetic Materials, 320(3–4):270–275.

[13]. Kosak, A., Makovec, D., Žnidaršič, A., Drofenik, M., 2004. Preparation of MnZn-ferrite with microemulsion technique. Journal of European Ceramic Society, 24(6): 959–962.

[14]. Takayama, A., Okuya, M., Kaneko, S., 2004. Spray pyrolysis deposition of NiZn ferrite thin films. Solid State Ionics, 172(1–4): 257–260.

[15]. Jiao, X., Chen, D., Hu Y., 2002. Hydrothermal synthesis of nanocrystalline $M_xZn_{1-x}Fe_2O_4$ (M=Ni, Mn, Co; x=0.40–0.60) powders. Materials Research Bulletin, 37(9): 1583–1588.

[16]. Zahra Rezay Marand, 2014. Study of magnetic and structural and optical properties of Zn doped Fe_3O_4 nanoparticles synthesised by coprecipitation method by biomedical application. Nanomedicine Journal, 1(4): 238-247.

[17]. Laokul, P., Amornkitbamrung, V., Seraphin, S., and Maensiri, S., 2011. Characterization and magnetic properties of nanocrystalline $CuFe_2O_4$, $NiFe_2O_4$, $ZnFe_2O_4$ powders prepared by the Aloe vera extract solution. Current Applied Physics, 11(1): 101–108.

[18]. Varma, R. S., 2012. Greener approach to nanomaterials and their sustainable applications. Current Opinion in Chemical Engineering, 1(2): 123–128.

[19]. Katewa, S.S., Chaudhary, B.L., Jain, A., 2004. Folk herbal medicines from tribal area of Rajasthan. India, Journal of Ethnopharmacology, 92(1): 41-46.

[20]. Balakrishnan, V., Prema, P., Ravindran, K.C., Robinson, J.P., 2009. Ethnobotanical studies among villagers from dharapuram taluk, tamil nadu, india. Global Journal of Pharmacology, 3(1): 8-14.

[21]. Jain, A., Katewa, S.S., Chaudhary, B.L., Galav, P., Folk herbal medicines used in birth control and sexual diseases by tribals of southern Rajasthan , India. Journal of Ethnopharmacology, 90(1): 171-177.

[22]. Leroy, J., 1978. Composition, origin, and affinities of the madagascan vascular flora. Annals of the Missouri Botanical Garden, 65(2): 535-589.

[23]. Shukla, Y.N., Khanuja, S.P.S., 2004. Chemical, pharmacological and botanical studies on Pedalium murex. Journal of medicinal and Aromatic Plant Sciences, 26(1): 64-69.

[24]. Pietta, P.G., 2000. Flavonoids as antioxidants. Journal of Natural products, 63(70000000): 1035-1042.

[25]. Jeyasundari et al, J., 2017. Green synthesis and characterization of zero valent iron nanoparticles from the leaf extract of psidum guajava plant and their antibacterial activity. Chemical Science Review and Letters, 6(22): 1244-1252.

[26]. Yousefi et al, A., 2015. Novel curcumin based pyrano (2, 3-d) pyrimidine antioxidant inhibitors for α-amylase and α-glycosidase: Implications for their pleiotropic effects, against diabetes complications. International journal of biological macromaolecules,78: 46-55.

[27]. Lahure et al, Preparation and characterization of zinc doped magnetite nanoparticles using green synthesis. International Journal of Research in chemistry and environment, 5(4): 60-64.

[28]. Wu, G., Tan, X., Li, G., Hu, C., 2010. Effect of preparation method on the physical and catalytic property of nanocrystalline Fe_2O_3. Journal of alloys and Compounds, 504: 371–376.

[29]. Elumalai et al, A., Reviw on therapeutic uses of pedalium murex. International Journal of Research in Ayurveda and pharmacy, 2(6): 1743-1745.

[30]. Anandalakshmi1et al, K., 2016. Characterization of silver nanoparticles by green synthesis method using pedalium murex leaf extract and their anti bacterial activity. Applied Nanoscience , 6: 399–408.